日本磁気学会
ISSN 2432-0250
Journal of the Magnetics Society of Japan
Electronic Journal URL: https://www.jstage.jst.go.jp/browse/msjmag

Vol.46 No.6　2022

Journal

Measurement Technique, High-Frequency Devices

Analysis of Demagnetizing Effects on Microstrip Line Type Probe for the Permeability Measurement of Thick Specimen

K. Takagi, M. Sakamoto, T. Ishihara, K. Okita, S. Yabukami, M. Yamaguchi, and K. Chatani　…102

JOURNAL OF THE MAGNETICS SOCIETY OF JAPAN

Vol.46 No.6 2022

日本磁気学会

ISSN 2432-0250

HP: http://www.magnetics.jp/ e-mail: msj@bj.wakwak.com
Electronic Journal: http://www.jstage.jst.go.jp/browse/msjmag

世界初！
高温超電導型VSM

新製品

世界初*、高温超電導マグネットをVSMに採用することで
測定速度 当社従来機1/20を実現。
0.5mm cube磁石のBr, HcJ高精度測定が可能と
なりました。
*2014年7月 東英工業調べ

測定結果例

高温超電導VSMによるNdFeB(sint.) 0.5mm cube BHカーブ

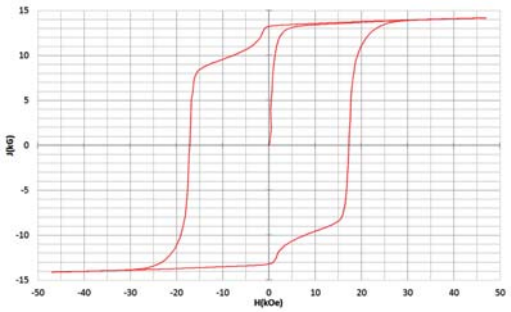

磁化測定レンジ：0.2emu
Br = 13.2kG　　HcJ = 17.2kOe

高温超電導VSMによるNdFeB(sint.) 1mm cube BHカーブ

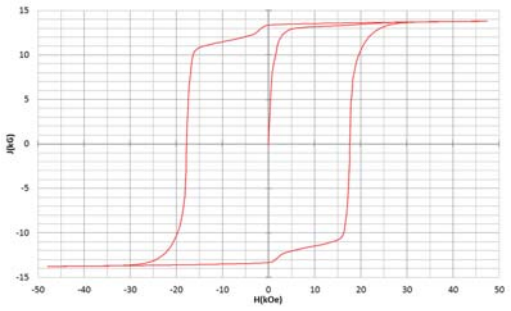

磁化測定レンジ：2emu
Br = 13.3kG　　HcJ = 17.7kOe

高温超電導VSMによるNdFeB(sint.) 4mm cube BHカーブ

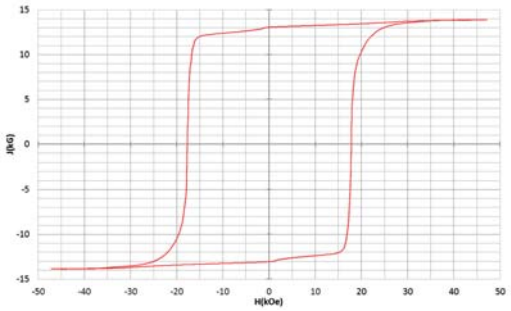

磁化測定レンジ：100emu
Br = 13.1kG　　HcJ = 17.8kOe

高速測定を実現

高温超電導マグネット採用により、高速測定を実現しました。Hmax= 5Tesla, Full Loop 測定が2分で可能です。
（当社従来機：Full Loop測定　40分）

小試料のBr,HcJ高精度測定

0.5mm cube 磁石のBr,HcJ高精度測定ができ、表面改質領域を切り出しBr,HcJの強度分布等、微小変化量の比較測定が可能です。
また、試料の加工劣化の比較測定が可能です。

試料温度可変測定

－50℃～＋200℃温度可変UNIT（オプション）

磁界発生部の小型化

マグネットシステム部寸法：0.8m×0.3m×0.3m

TOEI 東英工業株式会社
http://www.toeikogyo.co.jp
〒194-0035 東京都町田市忠生1-8-13
TEL：042-791-1211　FAX：042-792-0490
E-mail : sales@toeikogyo.co.jp

Journal of the Magnetics Society of Japan
Vol. 46, No. 6

Electronic Journal URL: https://www.jstage.jst.go.jp/browse/msjmag

CONTENTS

Measurement Technique, High-Frequency Devices

Analysis of Demagnetizing Effects on Microstrip Line Type Probe for the Permeability Measurement of Thick Specimen
.....K. Takagi, M. Sakamoto, T. Ishihara, K. Okita, S. Yabukami, M. Yamaguchi, and K. Chatani 102

J. Magn. Soc. Jpn., **46**, 102-106 (2022)

<Paper>

Analysis of Demagnetizing Effects on Microstrip Line Type Probe for the Permeability Measurement of Thick Specimen

K. Takagi*, M. Sakamoto**, T. Ishihara*, K. Okita**, S. Yabukami*,**, M. Yamaguchi*, ***, K. Chatani****

*Graduate school of Engineering, Tohoku Univ, *6-6-05 Aoba, Aramaki, Aoba-ku, Sendai 980-8579, Japan*

**Graduate school of Biomedical Engineering, Tohoku Univ., *6-6-05 Aoba, Aramaki, Aoba-ku, Sendai 980-8579, Japan*

***New Industry Creation Hatchery Center, Tohoku Univ., *6-6-10 Aoba, Aramaki, Aoba-ku, Sendai 980-8579, Japan*

****Advanced Materials R&D, TOKIN Corp., *6-7-1 Koriyama, Taihaku-ku, Sendai 982-8510, Japan*

This study analyzed the demagnetizing effect for a permeability measurement of a thick NiZn ferrite sheet (100 μm thickness) applied using a microstrip line type probe. The ferromagnetic resonance of the NiZn ferrite sheet was observed by two probes with different width conductors. The FMR frequency decreased as the offset between the microstrip conductor and the specimen increased. The two demagnetizing factors were estimated using the ferromagnetic resonance and FEM analysis, and the two values were almost equal. We simulated permeability using FEM, considering the intrinsic permeability of NiZn ferrite (evaluated using the Nicolson-Ross-Weir method) and the demagnetizing effect. The simulated permeability roughly corresponded with the measured value of the microstrip line type probe with a narrow conductor (0.36 mm wide). These results show that the demagnetizing effect is dominant for the high frequency permeability measurement of the thick specimen.

Key words: magnetic permeability, ferromagnetic resonance, magnetic film, demagnetizing factor

1. Introduction

The need to measure high frequency permeability of magnetic thin film has increased due to the rise in the usage of high frequency magnetic materials for the 5th generation mobile communication system, spintronic devices, etc. Many methods have been reported for evaluating the high-frequency magnetic permeability of magnetic materials and thin films[1)-13)]. Table 1 shows the comparison between our method and the others. The Nicolson-Ross-Weir (NRW) method is the standard and most popular method. However, the sample is strictly limited to a toroidal shape [5)]. The waveguide method has a very narrow frequency bandwidth and needs strip samples[14)].

Our microstrip line type (MSL) probe method enables ultra-wideband, high sensitivity, and sample size independent evaluation[15),16)]. However, since thick magnetic materials are placed close to the microstrip line conductor and the high frequency magnetic field is localized, there is the problem that the ferromagnetic resonance (FMR) frequency is shifted due to the demagnetizing effect[16)-18)]. Therefore, the purpose of this study is to analyze the shift of the FMR frequency due to the demagnetizing factor and to decrease the measurement error.

2. Demagnetizing effect of permeability measurement

The demagnetizing effect is a common phenomenon occurred by exciting some portions of a sample. In our microstrip line type (MSL) probe, the magnetic field is localized near the microstrip line, so the effect of the demagnetizing field is very obvious. Two kinds of demagnetizing factors should be considered when using the MSL probe to measure the permeability of magnetic films. The first factor is the width of the microstrip line. The second factor is the concentration of high frequency current in the microstrip conductor due to the eddy current effect[19)]. It is recognized that both factors can enlarge the demagnetizing effect. According to Muroga[20)], the demagnetizing factor, N_d, is suggested to become smaller in order to measure magnetic permeability accurately. Otherwise, a frequency shift of the FMR might occur.

Equation (1) shows the relation between the FMR frequency, f_{fmr}, and an anisotropy field, H_k. Here, γ is the gyromagnetic constant, M_s the magnetization of magnetic film, and μ_0 is the permeability of air.

$$f_{fmr} = \frac{\gamma}{2\pi}\sqrt{\frac{M_s H_k}{\mu_0}} \quad (1)$$

Table 1 Comparison of selected methods. The MSL probe method has some superior features, such as having a wide frequency band and being capable of measuring samples without size limitation.

Method	MSL probe method	The Nicolson-Ross-Weir (NRW) method[5)]	The Waveguide method[14)]
Accuracy	Medium	Precise	Precise
Band range	Extremely wide (up to 67 GHz)	Medium range	Narrow range
Sample shape	Free from sample size limitation (up to 12" wafer)	Toroidal shape	Strip shape

Corresponding author: K. Okita
(kazuhiko.okita.b5@tohoku.ac.jp)

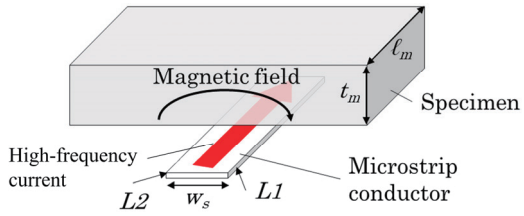

Fig. 1 Configuration of MSL probe.

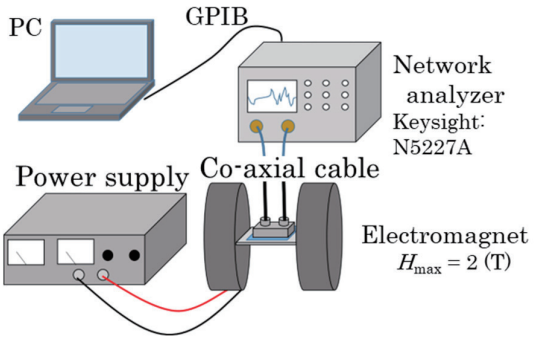

Fig. 2 Schematic diagram of the measurement system. A network analyzer is the main instrument for measuring S parameters in the wide range of 10 MHz to 67 GHz.

If the demagnetizing factor is negligibly small, FMR frequency can be obtained by the equation (1).

Fig. 1 shows a configuration of the MSL probe and a specimen. A high-frequency magnetic field is applied to a specimen using a current flowing in the microstrip line. The N_d increased as the width of the microstrip line, w_s, decreased[21] at higher frequencies.

3. Analysis and Experiments

Fig. 2 shows a schematic diagram of the experimental procedure. The main piece of equipment is a network analyzer (N5227A) capable of measuring a wide frequency range of 10 MHz to 67 GHz. The output power was 10 dBm and a magnetic field around 1 A/m or less was applied to the specimen. The electromagnet applied the DC magnetic field up to 2 T which was enough strong to almost completely saturate soft magnetic material. Fig. 3 shows the MSL probes, designed to measure a wide frequency up to 67 GHz with the microstrip conductor with widths of 0.36 mm and 1.2 mm.

Fig. 4 shows a flow chart to measure and obtain magnetic permeability. First, the sample was set in the proximity of the microstrip conductor. Second, the transmission coefficient, S_{21}, was calibrated in a strong magnetic field around 2 T as a reference. Third, the S_{21} was measured without a magnetic field in the main measurement and obtained the equivalent impedance of the sample, Z_s. The complex permeability was optimized using FEM analysis and the equivalent impedance, Z_s. The equivalent impedance was

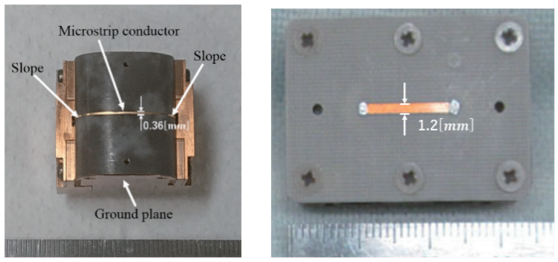

Fig. 3 Photo of the MSL probe. This probe has a narrow microstrip line (0.36 mm wide (left)[16] and 1.2 mm wide (right)[22]) and copper block as return pass.

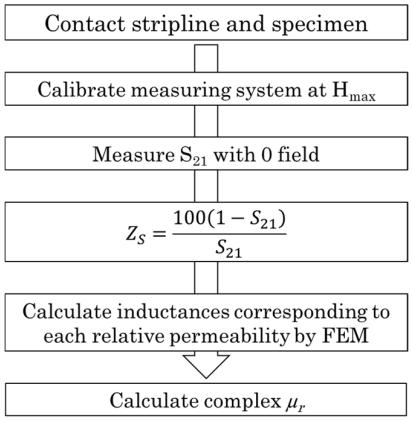

Fig. 4 Flow chart of the experimental procedure. S_{21}, transmission coefficients, are measured first. From this, the permeability is calculated.

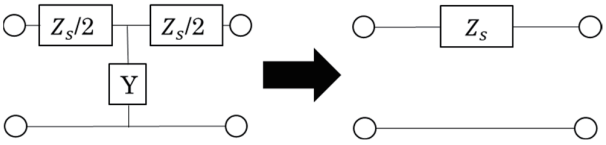

Fig. 5 Equivalent circuit for measuring sample. By calibrating network analyzer at strong enough field to saturate sample, the equivalent circuit is simplified as shown in above right.

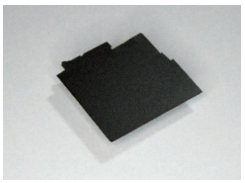

Fig. 6 Photograph of NiZn ferrite film. This sheet is around 0.1 mm thick, and ferrite particles are contained in the polyethylene film[23].

transferred from the circuit as shown in Fig. 5. The complex permeability can be obtained from the impedance, Z_s because it can ignore admittance, Y.

Fig. 6 shows a photograph of the NiZn ferrite sheet produced by the Tokin corporation. The dimensions of the sample were 0.1 mm (thickness) x 10 mm (width) x 10 mm (length).

4. Experimental and theoretical results

Fig. 7 shows the measured FMR frequency as a

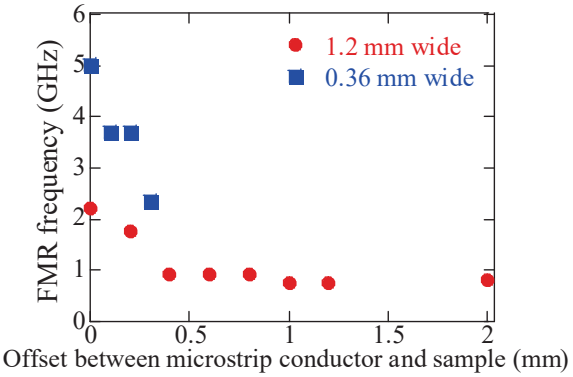

Fig. 7 The FMR frequency as a function of the offset between the microstrip conductor and the sample (NiZn ferrite sheet).

function of the offset between the microstrip conductor and the sample (the NiZn ferrite sheet). The FMR frequency decreased by increasing the offset between the microstrip conductor and the sample. The FMR frequency measured by a 0.36 mm wide conductor was higher than that measured with a 1.2 mm wide conductor. This suggested that the demagnetizing effect in the narrow microstrip conductor is more dominant than that in the wide conductor. An almost intrinsic FMR frequency of about 0.9 GHz was observed using the 1.2 mm wide probe when the offset was over 0.4 mm because the demagnetizing effect was negligibly small. The FMR frequency was estimated to be approximately 0.9 GHz using equation (1), which was derived from the Landau-Lifshitz-Gilbert equation.

Therefore, we analyzed the demagnetizing effect using two approaches. Table 2 shows the comparison of the demagnetizing factor from the FMR frequency and from the FEM analysis. At first, the magnetizing factor of the microstrip line and thick sample was estimated using two-dimensional FEM analysis. Fig. 8 shows a model for the FEM simulation. The FEM analysis was performed using a commercial solver (Maxwell, Ansoft co. Ltd.). The frequency was 1 GHz, and the relative permeability of the sample was 3, which corresponded to the intrinsic relative permeability of the NiZn ferrite sheet[23]. The imaginary part of the permeability was neglected in the FEM analysis. Fig. 9 (a) and (b) shows the calculated flux lines when the width of the microstrip conductor was 0.36 mm and 1.2 mm, respectively. The demagnetizing factor, N_d, was obtained using equation (2) [24] along the "y" axis in Fig. 8,

$$N_d = \frac{H(\mu_r = 1) - H(\mu_r)}{\chi H(\mu_r)} \qquad (2)$$

where $H(\mu_r=1)$ is the magnetic field when the relative permeability of the sample was 1, $H(\mu_r)$ is the magnetic field when the relative permeability was μ_r, and κ is

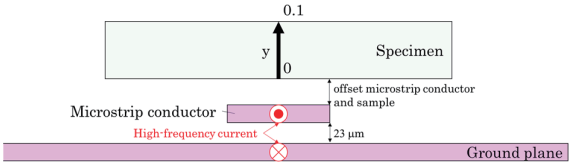

Fig. 8 Calculation model and evaluation of the demagnetizing factor. "*y*" is the distance from the center point of the specimen on the side of strip line to the opposite surface, the thickness of which is assumed to be 0.1 mm.

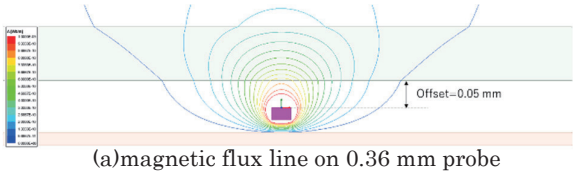

(a)magnetic flux line on 0.36 mm probe

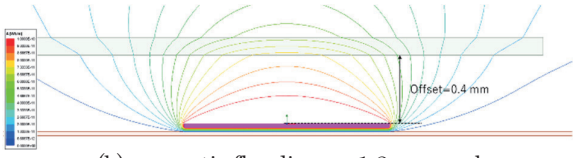

(b) magnetic flux line on 1.2 mm probe

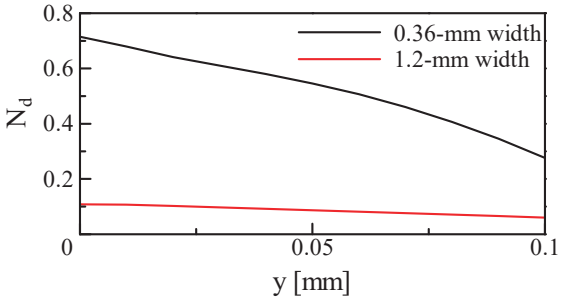

(c) distribution of N_d

Fig. 9 Calculated lines of flux and distribution of N_d. These values are calculated using FEM along the center line "y" of the specimen.

Table 2 Comparison of the demagnetizing factor between from the FMR frequency and FEM analysis.

Microstrip conductor width (mm) / offset (mm)	0.36/0.05	1.20/0.4
FMR frequency (GHz)	5.0	0.9
demagnetizing factor from FMR	0.586	0.087
demagnetizing factor from FEM	0.524	0.082

the magnetic susceptibility. From the FEM analysis of Fig. 8 and 9, the average N_d are obtained to be 0.082 and 0.524 for the 0.36 mm and 1.2 mm width probes, respectively.

In Table 2, another demagnetizing factor was estimated from the ferromagnetic resonance frequency obtained using Fig. 9 and equation (3).

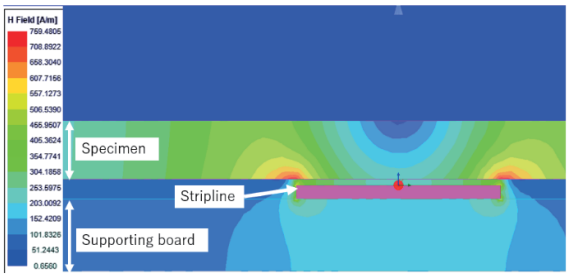

Fig. 10 Simulation of magnetic field. Two high field areas are observed near the edge of the strip line on the sample surface.

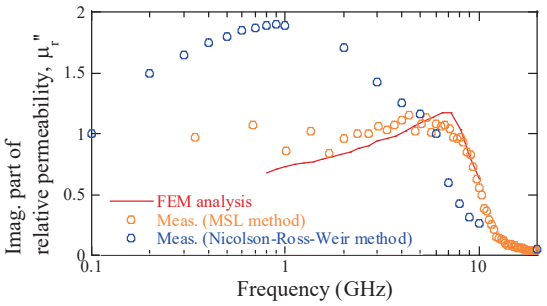

Fig. 11 Simulated μ_r" using FEM and measured data. The solid line is calculated using FEM and the square symbols show the data measured with the NRW method for comparison. The simulation predicted the shift of the FMR frequency. The measured spectrum using an MSL probe roughly agreed with the simulation data.

$$f_{fmr} = \frac{\gamma}{2\pi}\sqrt{\frac{M_s(H_k + N_d M_s)}{\mu_0}} \qquad (3)$$

where M_s, H_k, and γ of NiZn ferrite were 183 kA/m, 3.58 kA/m, and 2.21x10^5 [25), 26)], respectively. A demagnetizing factor of 0.524 and 0.082 was obtained respectively. The demagnetizing factors from the FMR frequency agreed with those derived from the FEM analysis. This means that the demagnetizing effect increased the FMR frequency when the 0.36 mm wide probe was applied to the thick specimen. In the 1.2 mm wide probe, an adequate offset (over 0.4 mm) released the demagnetizing effect and can evaluate the intrinsic FMR frequency even if the thickness of the specimen increased to about 0.1 mm.

Fig. 10 shows a contour diagram of the magnetic field calculated using FEM when a high-frequency current at 1 GHz flows in the microstrip line. It can be found that the strong RF magnetic fields localized near the edges of the microstrip line (the red area of the specimen), which resulted in the demagnetizing effect.

Fig. 11 shows a comparison between the simulated and measured permeability of the NiZn ferrite sheet (0.1 mm thick) using the 0.36 mm wide microstrip probe. The measured permeability using the Nicolson-Ross-Weir method is also present in the graph. As we mentioned in Fig. 7, the demagnetizing effect was dominant using the probe. Therefore, the measured FMR frequency shifted about 5 GHz, which was higher than that of the Nicolson-Ross-Weir method[16]. The FEM simulation was performed using HFSS (ANSYS Electronics Desktop 2020R1). The measured permeability from the Nicolson-Ross-Weir method was used for comparison to the FEM analysis. The procedure to obtain the permeability from the FEM analysis is the same as the experimental one in Fig. 4. The FEM analysis was considered for the demagnetizing effect of the specimen. As shown in Fig. 11, the simulated permeability roughly agreed with the measured permeability. Therefore, we successfully analyzed that the ferromagnetic resonance frequency shift and the measurement error of permeability were caused by the demagnetizing effect.

5. Conclusion

1. This paper presents the analysis of the demagnetizing effect which is dominant for high-frequency permeability measurement of thick NiZn ferrite.
2. Two microstrip line type probes with different width conductors were prepared in order to measure the ferromagnetic resonance of the NiZn ferrite sheet. The FMR frequency decreased as the offset between the microstrip conductor and the sample increased. The demagnetizing effect in the narrow microstrip conductor was more dominant than in the wide conductor.
3. The demagnetizing factors in the different probes were estimated using the FEM analysis and FMR frequency. Both demagnetizing factors corresponded. The localization of the RF magnetic field around the edge of the microstrip conductor caused the demagnetizing effect dominantly.
4. We simulated permeability using FEM, considering the intrinsic permeability of NiZn ferrite and the demagnetizing effect. The simulated permeability roughly corresponded to the measured value using the narrow MSL method.

Acknowledgements We would like to thank Prof. S. Saito and his team at Tohoku Univ. for helping us use the electromagnet to measure magnetic permeability. This work was supported in part by research and development for expansion of radio-wave resources from the Ministry of Internal Affairs and Communications of Japan (JPJ000254), the NEDO Entrepreneurs Program (0329006), the JST A-step tryout program (JPMJTM22AB) and the Joint Development Research 2022-ACCL-1 at High Energy Accelerator Research Organization (KEK).

References

1) P. A. Calcagno and D. A. Thompson: *Rev. Sci. Instrum.*, **46**, 904 (1975).
2) M. Yamaguchi, S. Yabukami, and K. I. Arai: *IEEE Trans. Magn.*, **32**, 4941 (1996).
3) M. Yamaguchi, S. Yabukami and K. I. Arai: *IEEE Trans. Magn.*, **33**, 3619 (1997).
4) H. B. Weir, *Proc IEEE*, **62**, 33 (1975).
5) A. M. Nicolson and G. F. Ross: *IEEE Trans. Instrum. Meas.*: **19**, 377 (1970).
6) T. Kimura, M. Mitera, M. Terasaka, M. Nose, F. Futamoto, H. Matsuki, H. Fujimori and T. Masumoto: *J. Magn. Soc. Jpn.*, **17**, 497 (1993).
7) G. Counil, J. V. Kim, T. Devolder, C. Chappert, K. Shigeto and Y. Otani: *J. Appl. Phys*, **95**, 5646(2004).
8) P. Queffelec, P. Gelin, J. Gieraltowski and J. Loäec: *IEEE Trans. Magn.*, **30**, 224 (1994).
9) M. Senda and O. Ishii: *IEEE Trans. Magn.*, **31**, 960 (1995).
10) V. Korenivski, R. B. van Dover, P. M. Mankiewich, Z. -X. Ma, A. J. Becker, P. A. Polakos and V. J. Fratello: *IEEE Trans. Magn.*, **32**, 4905 (1996).
11) Y. Yip, M. J. Vos, M. Lu, M. P. Dugas and J. H. Judy: *IEEE Trans. Magn.*, **24**, 3072 (1988).
12) A. Yoshihara, K. Takanashi, M. Shimoda, O. Kitakami and Y. Shimada: *Jpn. J. Appl. Phys*, **33**, 3927 (1994).
13) S. Bie, J. Jiang, G. Du, Q. Ma, L. Yuan, Y. Di, Z. Feng and H. He: *J. Alloys Compd.*, **463**, 471 (2008).
14) T. Miura, and K. Tahara, *IEEE Trans. Microwave Theory and Techniques*, **68**, 1773 (2020).
15) S. Yabukami, K. Nozawa, L. Tonthat, K. Okita, and S. Ranajit: *IEEE Tran. Magn.*, **57**, 6100405 (2021).
16) S. Yabukami, C. Iwasaki, K. Nozawa, S. Takahashi, K. Okita, K. Chatani: *IEEE Trans. Magn.*, **58**, 1 (2022).
17) G.Q. Lin, Z.W. Li, Linfeng Chen, Y.P. Wu, C.K. Ong: *J. Magn. Magn. Mater.*, **305**, 291 (2006).
18) O. Kohmoto: *J. Magn. Magn. Mater.*: **262**, 280 (2003).
19) M. Yamaguchi, and Miyazawa: *Oral session of the 45th Annual Conf. on Magn. in Japan*, (01aC-4), Sept.1 (2021).
20) S. Muroga, Y. Asazuma, and M. Yamaguchi: *IEEE Trans. Magn.*, **49**, 4032 (2013).
21) S. Muroga, Y. Endo, Y. Mitsuzuka, Y. Shimada and M. Yamaguchi: *IEEE Trans. Magn.*, **47**, 300 (2011).
22) T. Kimura, S. Yabukami, T. Ozawa, Y. Miyazawa, H. Kenju, Y. Shimada: *J. Magn. Soc. Jpn.*, **38**, 87 (2014).
23) JFE TECHNICAL REPORT, **26**, 77 (2010).
24) K. Ohta: Jikikogaku no Kiso 1 (in Japanese), p. 198 (Kyoritsu Shuppan, Tokyo, 1973).
25) S. Chikazumi: Kyojiseitai no Butsuri 2nd volume (in Japanese), p. 324 (Shokabo, Tokyo, 1984).
26) P. Zhou, M. A. Popov, Y. Liu, R. Bidthanapally, D. A. Filippov, T. Zhang, Y. Qi, P. J. Shah, B. M. Howe, M. E. McConney, Y. Luo, G. Sreenivasulu, G. Srinivasan and M. R. Page: *Phys. Rev. Mater.*, **3**, 044403 (2019).

Received Nov. 09, 2021; Revised Jun. 13, 2022; Accepted Aug. 30, 2022

Journal of the Magnetics Society of Japan

Vol. 46 No. 6 (通巻第324号) 2022年11月1日発行

Vol. 46 No. 6 Published Nov. 1, 2022
by the Magnetics Society of Japan
Tokyo YWCA building Rm207, 1–8–11 Kanda surugadai, Chiyoda-ku, Tokyo 101–0062
Tel. +81–3–5281–0106 Fax. +81–3–5281–0107

Printed by JP Corporation Co., Ltd.
Sports Plaza building 401, 2–4–3, Shinkamata Ota-ku, Tokyo 144–0054
Advertising agency: Kagaku Gijutsu-sha

発行：(公社)日本磁気学会 101–0062 東京都千代田区神田駿河台 1–8–11 東京YWCA会館 207 号室
製作：ジェイピーシー 144–0054 東京都大田区新蒲田 2–4–3 スポーツプラザビル401 Tel.（03）6715–7915
広告取扱い：科学技術社 111–0052 東京都台東区柳橋 2–10–8 武田ビル 4F Tel.（03）5809–1132